

Quantum Noise of Kramers-Kronig Receiver

FAN ZHANG,^{1,4} JIAYU ZHENG,¹ HAIJUN KANG,² XIAOLONG SU,² AND QIONGYI HE³

¹ State Key Laboratory of Advanced Optical Communication System and Networks, Frontiers Science Center for Nano-optoelectronics, Department of Electronics, Peking University, Beijing 100871, China

² State Key Laboratory of Quantum Optics and Quantum Optics Devices, Institute of Opto-Electronics, Collaborative Innovation Center of Extreme Optics, Shanxi University, Taiyuan 030006, China

³ State Key Laboratory for Mesoscopic Physics, School of Physics, Frontiers Science Center for Nano-optoelectronics & Collaborative Innovation Center of Quantum Matter, Peking University, Beijing 100871, China

⁴ Peng Cheng Laboratory, Shenzhen 518055, China.

*xyz@optica.org

Abstract: The Kramers-Kronig (KK) receiver provides an efficient method to reconstruct the complex-valued optical field by means of intensity detection given a minimum-phase signal. In this paper, we analytically show that for detecting coherent states, quantum noise of the KK receiver keeps the radical fluctuation of measuring the minimum-phase signal, the same as the balanced heterodyne detection does, while compressing the tangential fluctuation to 1/3 times the radical one using information provided by the Hilbert transform. In consequence, the KK receiver achieves 3/2 times the signal-to-noise ratio of balanced heterodyne detection, while presenting an asymmetric quantum fluctuation distribution depending on the time-varying phase. This further provides a feasible scheme for compressing the quantum fluctuation of measuring the coherent state in a specific direction to 1/6, which is even lower than 1/4 of measuring directly in the same direction. Our work presents a physical insight of the KK receiver and a further step of deep understanding of electromagnetic noise in quantum optical measurement.

© 2021 Optica Publishing Group under the terms of the [Optica Publishing Group Open Access Publishing Agreement](#)

1. INTRODUCTION

Optical receiver can be categorized as two basic schemes of coherent and direct detections [1]. Coherent receiver can either use homodyne or heterodyne detection to retrieve the complexed full field information of the received signals. In contrast, direct detection can only obtain the signal intensity due to the square-law principle. Recently, an advanced concept of Kramers-Kronig (KK) receiver was proposed [2, 3], which can reconstruct the complex-valued optical field by means of intensity detection given a minimum-phase (MP) signal. For the KK receiver applied on the MP signal, the amplitude waveform determines its corresponding phase waveform uniquely up to a constant phase offset. The physical mechanism is that the logarithm of the signal intensity and phase are related to each other through the KK relations that apply to the signals that are causal in time. For a MP signal, it contains a data-carrying signal and a reference component that is a continuous-wave tone. When the spectrum of the signal's complex envelope is entirely above or below the reference frequency, which is so called single-sideband (SSB) signal, then a necessary and sufficient condition to be of minimum-phase is that its time-domain trajectory never encircles the origin of the complex plane. From the point of the configuration, the KK receiver is equivalent to heterodyne detection with one single photodetector (PD). Due to the fact that the receiver optical front-end consists of a single photodetector, the KK receiver is particularly suitable for low-cost data center interconnect and metro-haul applications [4]. In this way, high baud rate quadrature amplitude modulation (QAM) signal can be detected using a single PD at the receiver [5].

Quantum noise, which comes from the uncertainty principle of quantum variables, sets a limitation for the signal-to-noise ratio (SNR) in the measurement of an optical signal. In quantum information with

continuous variables, the information is encoded in the amplitude and phase components of optical modes and measured by homodyne or heterodyne detection [6-10]. For heterodyne detection, a simultaneous measurement of two noncommuting quantum observables introduces excess noise that originates from vacuum fluctuations of the field, which imposes a fundamental limit on the SNR [11]. The KK receiver offers a simultaneous measurement of the in-phase and quadrature components of the optical field, which corresponds to the amplitude and phase quadratures of an optical mode in quantum optics. A natural question is how about the quantum noise of the KK receiver?

In this paper, we study the quantum mechanical nature of the KK receiver and elucidate the fundamental relation between the KK receiver and the conventional balanced heterodyne detection. The result shows that the KK detection achieves 3/2 times the SNR of the balanced heterodyne detection. Interestingly, the quantum noise of the KK receiver shows an asymmetric fluctuation distribution, which is different from that of the balanced heterodyne detection. In this case, quantum noise of the KK receiver is time dependent for the in-phase and quadrature operators of an optical field, which corresponds to the amplitude and phase quadratures of an optical mode in quantum optics. Our result indicates the quantum noise limit and fluctuation properties of the KK receiver when it is used to measure the coherent state.

2. QUANTUM MECHANICAL FUNDAMENTALS OF COHERENT STATE

For optical transmission, information is conveyed by electromagnetic wave packets those are quantum states of the electromagnetic field. A signal carried by the coherent state $|\alpha_s\rangle$ is the eigenfunction of the photon annihilation operator \hat{a} , which is expressed as $\hat{a}|\alpha_s\rangle = \alpha_s|\alpha_s\rangle$. With the Hermitian conjugate

operation, the creation operator satisfies $\langle \alpha_s | \hat{a}^\dagger = \alpha_s^* \langle \alpha_s |$, thus the photon number n satisfies $\langle n_s \rangle = |\alpha_s|^2$. The non-Hermitian operator \hat{a} can be separated into two Hermitian components \hat{X} and \hat{Y} by $\hat{a} = \hat{X} + j\hat{Y}$, which are the in-phase and quadrature field operators and satisfy the commutation relation given by $[\hat{X}, \hat{Y}] = j/2$. Here,

$\hat{X} = \sqrt{\frac{\omega}{2\hbar}} \hat{q}$ and $\hat{Y} = \frac{\hat{p}}{\sqrt{2\hbar\omega}}$ are essentially dimensionless position

and momentum operators, which correspond to the amplitude and phase quadratures of an optical mode in quantum optics, respectively.

The Heisenberg uncertainty principle sets an upper limit on the precision of a quantum measurement. We assume that $\langle (\Delta\hat{X})^2 \rangle$ represents the quantum variance of measuring the observable \hat{X} . The coherent state is one of the minimum uncertainty states, of which the quantum variances of the in-phase and quadrature operators are $\langle (\Delta\hat{X})^2 \rangle = 1/4$ and $\langle (\Delta\hat{Y})^2 \rangle = 1/4$, respectively. Thus, the total variance is $\langle (\Delta\hat{a})^2 \rangle = \langle (\Delta\hat{X})^2 \rangle + \langle (\Delta\hat{Y})^2 \rangle = 1/2$ [11, 12].

The quantum variances of the amplitude and phase of a coherent state are $\langle (\Delta|\hat{a}|)^2 \rangle = 1/4$ and $\langle (\Delta\hat{\phi})^2 \rangle = 1/(4\langle n \rangle)$, respectively [12]. Here the photon number n satisfies $\langle n \rangle = |\alpha|^2$. For any coherent state $|\alpha\rangle$ that has a time dependence $e^{-j\omega t}$, its corresponding annihilation operator is defined as $\hat{A}|\alpha\rangle = e^{-j\omega t}\alpha|\alpha\rangle$. \hat{A} and its conjugate operator \hat{A}^\dagger obey the commutation relation $[\hat{A}, \hat{A}^\dagger] = 1$.

3. QUANTUM MECHANICS MODEL OF BALANCED HETERODYNE DETECTION

As shown in Fig. 1 (a), the balanced heterodyne detection is adopted to get the linear beating between the local oscillator (LO) \hat{A}_L at frequency ω_L and the signal \hat{A}_s at frequency ω_s . The waves \hat{B}_1 and \hat{B}_2 that incident upon the two PDs are

$$\hat{B}_1 = \frac{1}{\sqrt{2}} [\hat{A}_L + \hat{A}'_s + \hat{A}'_i - j(\hat{A}_s + \hat{A}_i)], \quad (1)$$

$$\hat{B}_2 = \frac{1}{\sqrt{2}} [-j(\hat{A}_L + \hat{A}'_s + \hat{A}'_i) + (\hat{A}_s + \hat{A}_i)]. \quad (2)$$

Here \hat{B}_1 and \hat{B}_2 have considered the signal \hat{A}_s at frequency ω_s and its image \hat{A}_i at $\omega_i = 2\omega_L - \omega_s$, as well as the vacuum fluctuations \hat{A}'_s and \hat{A}'_i at these two frequency points brought by LO as shown in Fig. 1 (a). Note that n photons are received by the photodetector within the signal duration T . With the elementary charge q , the current is $\hat{I} = q\hat{n}/T$. The difference between the current collected by the two detectors is

$$\begin{aligned} \langle \hat{I}(t) \rangle_{Bal} &= k \langle \hat{B}_2^\dagger \hat{B}_2 - \hat{B}_1^\dagger \hat{B}_1 \rangle \\ &= 2k |\alpha_s \alpha_L^*| \sin(\omega_{IF} t - \arg(\alpha_s \alpha_L^*)). \end{aligned} \quad (3)$$

Here $k = q/T \cdot \alpha_s$ and α_L are the eigenvalues for the signal and the LO, respectively. $\omega_{IF} = \omega_s - \omega_L$ is the intermediate frequency. For the image band, there exists that $\langle \hat{A}_i^\dagger \hat{A}_i \rangle = 0$. Yet the presence of \hat{A}_i contributes to the fluctuations. The variance of photocurrent is given by

$$\langle (\Delta\hat{I})^2 \rangle_{Bal} = \langle \hat{I}(t)^2 \rangle - \langle \hat{I}(t) \rangle^2 = k^2 (3\langle n_s \rangle + 2\langle n_L \rangle). \quad (4)$$

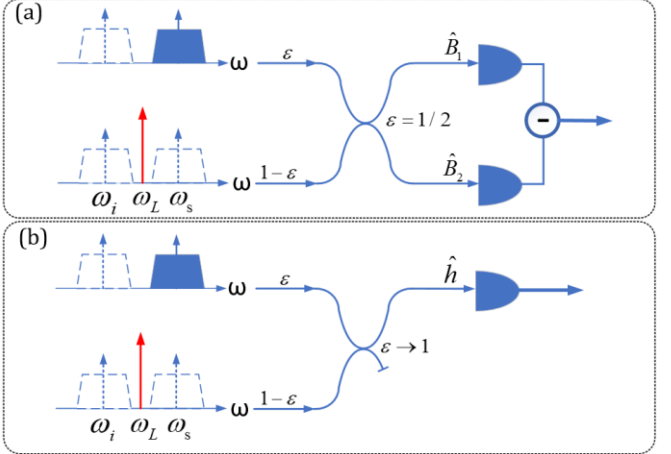


Fig. 1. Basic configurations of the balanced heterodyne and KK detection. (a) Balanced heterodyne detection; (b) The KK detection.

Then the S/N of the balanced heterodyne detection is calculated from Eq. (3) and (4), which is given by

$$(S/N)_{Bal} = \frac{\langle \hat{I}(t) \rangle_{Bal}^2}{\langle (\Delta\hat{I})^2 \rangle_{Bal}} = \frac{2\langle n_s \rangle \langle n_L \rangle}{2\langle n_L \rangle + 3\langle n_s \rangle} = \frac{\langle n_s \rangle}{1 + 3\langle n_s \rangle / 2\langle n_L \rangle}. \quad (5)$$

Here the operation “ $\hat{X}(t)$ ” means averaging the value $\hat{X}(t)$ by time.

4. QUANTUM MECHANICS MODEL OF THE KK RECEIVER

For the KK receiver, the signal is retrieved with one single PD of the balanced detection, which is equivalent to sending the LO along with the signal from the transmitter side as shown in Fig. 1 (b). The MP signal is constructed with a co-polarized reference carrier with real-valued amplitude and a complexed optical data. When the MP signal impinges upon one single PD, the beating between the reference carrier and the data-carrying signal is analogue to heterodyne detection.

Without loss of generality, we express the MP signal as $h(t) = \sqrt{1-\varepsilon} A_L + \sqrt{\varepsilon} A_s(t)$ depicted in Fig. 1 (b), where the power transmission ε is set to $\frac{1}{2}$ for balanced detection in Fig. 1 (a). For the KK receiver, in order to maximize the utilization of signals, we set the power transmission $\varepsilon \rightarrow 1$. Considering the fast time-vary phase of the optical carrier, we rewrite the MP signal as $h(t) = [\sqrt{1-\varepsilon} \alpha_L + \sqrt{\varepsilon} \alpha_s(t) e^{-j\omega_{IF} t}] e^{-j\omega_L t}$. For a complex data-carrying signal $\alpha_s(t)$ whose spectrum is contained in the frequency range $(0, W]$, an ideal SSB signal that has its spectrum closely above

the reference frequency ω_L satisfies $\omega_{IF} = \pi W$. The second-order term $\varepsilon |\alpha_s(t)|^2$ is commonly referred to as the signal-to-signal beat interference (SSBI) [3], whose spectrum is in the frequency of $[-W/2, W/2]$. The balanced heterodyne detection can eliminate SSBI by the subtraction in Eq. (3). In contrast, for the KK receiver that with one single PD, the SSBI cancellation is not required as $\varepsilon |\alpha_s(t)|^2$ is an essential part of the detected current intensity that required for the reconstruction [3].

For each signal transmitted, the purpose of KK receiver is to recover the baseband signal $\alpha_s(t)$ at the decision time t from the amplitude and phase of $h(t)$. The current $I(t) = k |h(t)|^2$ is obtained from a single PD. With the MP condition $\varepsilon \langle n_s \rangle < (1-\varepsilon) \langle n_L \rangle$, the phase of $h(t)$ that can be extracted from the current logarithm with Hilbert transform is defined as [2]

$$\phi(t) = \frac{1}{2\pi} \mathcal{P} \int_{-\infty}^{+\infty} \frac{\ln |I(t')|}{t-t'} dt'. \quad (6)$$

Here \mathcal{P} represents the Cauchy principal value. The complex signal field α_s is retrieved as α'_s .

$$\alpha'_s = \left[\frac{1}{\sqrt{\varepsilon}} |h(t)| e^{j\phi(t)} - \frac{\sqrt{1-\varepsilon}}{\sqrt{\varepsilon}} \sqrt{\langle n_L \rangle} \right] e^{j\omega_{IF} t}. \quad (7)$$

The relation between α'_s and $h(t)$ is shown in Fig. 2, in which $\phi(t)$ is the time-varying phase difference between $h(t)$ and $\sqrt{1-\varepsilon} \alpha_L$.

From Eq. (7), the relation between $\Delta\hat{\alpha}'_s$ and $\Delta\hat{h}$ is given by multiplying the phase factor $e^{j\omega_{IF} t}$.

$$\Delta\hat{\alpha}'_s = \Delta\hat{h} e^{j\omega_{IF} t}. \quad (8)$$

It is obvious that the retrieved α'_s , which can be obtained from $h(t)$ after a phase shift with an exponent translation, has the quantum noise determined by that of $h(t)$. Therefore, we study the quantum fluctuations of α'_s through those of $h(t)$ in the case of KK detection.

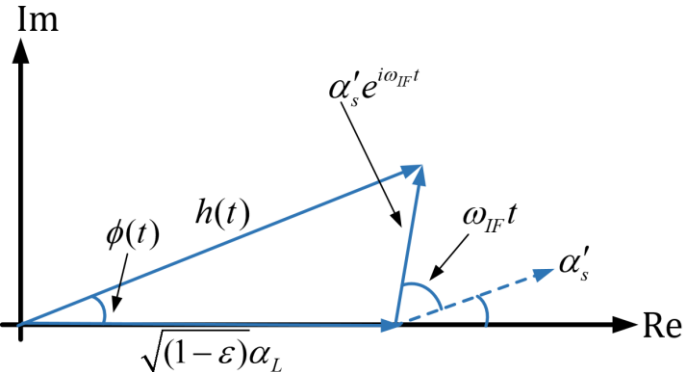


Fig. 2. The relationship between the retrieved α'_s and $h(t)$ for KK detection.

Considering the signal and its image, as well as their corresponding vacuum fluctuations brought by the carrier [11], we have $\hat{h} = \sqrt{1-\varepsilon}(\hat{A}_L + \hat{A}'_s + \hat{A}'_i) + \sqrt{\varepsilon}(\hat{A}_s + \hat{A}_i)$ before the PD

port as shown in Fig. 1 (b), in which the operators \hat{A}_L , \hat{A}'_s , \hat{A}'_i , \hat{A}_s & \hat{A}_i are all for single frequency.

Note that $I(t)$ corresponds to the photocurrent expectation $\langle \hat{I}(t) \rangle_{KK}$, which is obtained by projection via the coherent states, product states of the LO and the signal (and its image) states.

$$\begin{aligned} \langle \hat{I}(t) \rangle_{KK} &= k \langle \hat{h}^\dagger \hat{h} \rangle = k \langle \alpha_L | \langle \alpha_s | \langle \alpha_i | \hat{h}^\dagger \hat{h} | \alpha_i \rangle | \alpha_s \rangle | \alpha_L \rangle \\ &= k [\varepsilon \langle n_s \rangle + (1-\varepsilon) \langle n_L \rangle \\ &\quad + 2\sqrt{\varepsilon(1-\varepsilon)} |\alpha_s \alpha_L^*| \cos(\omega_{IF} t - \arg(\alpha_s \alpha_L^*))]. \end{aligned} \quad (9)$$

The mean variance of the photocurrent is given by

$$\begin{aligned} \langle (\Delta\hat{I}(t))^2 \rangle_{KK} &= \langle \hat{I}(t)^2 \rangle - \langle \hat{I}(t) \rangle^2 \\ &= 2k^2 [\varepsilon \langle n_s \rangle + (1-\varepsilon) \langle n_L \rangle \\ &\quad + 2\sqrt{(1-\varepsilon)\varepsilon} |\alpha_s \alpha_L^*| \cos(\omega_{IF} t - \arg(\alpha_s \alpha_L^*))]. \end{aligned} \quad (10)$$

The fluctuations of the photon current are related to the operators $\hat{A}_i \hat{A}_i^\dagger$, $\hat{A}_s \hat{A}_s^\dagger$ and $\hat{A}_L \hat{A}_L^\dagger$, which are in reverse order to the photon number operator. It is worth noting that the ratio of $\langle (\Delta\hat{I}(t))^2 \rangle_{KK}$ to $\langle \hat{I}(t) \rangle_{KK}$ is a constant $2k$. A general mathematical proof is given in the Supplement, Note 1.

The operator $\Delta\hat{\phi}(t)$ representing the difference between the measured phase $\hat{\phi}(t)$ and the expected phase $\phi(t)$, which is obtained after Taylor expansion and approximation of the logarithm function in Eq. (6), is expressed by

$$\Delta\hat{\phi}(t) = \hat{\phi}(t) - \phi(t) \approx \frac{1}{2\pi} \mathcal{P} \int_{-\infty}^{+\infty} \frac{1}{t-t'} \frac{[\hat{I}(t') - I(t')]}{I(t')} dt'. \quad (11)$$

The phase fluctuations $\langle (\Delta\hat{\phi}(t))^2 \rangle$ can be expressed in discrete form with $t = l\delta t$, $t' = m\delta t$ and $dt' \rightarrow \delta t$.

$$\begin{aligned} \langle (\Delta\hat{\phi}(t))^2 \rangle &= \lim_{\delta t \rightarrow 0} \frac{1}{4\pi^2} \left[\sum_{m=-\infty, m \neq l}^{m=+\infty} \frac{1}{(l-m)^2} \frac{\langle (\Delta\hat{I}(m\delta t))^2 \rangle}{I(m\delta t)^2} \right] \\ &= \lim_{\delta t \rightarrow 0} \frac{1}{12} \frac{\langle (\Delta\hat{I}(t))^2 \rangle}{(I(t))^2} = \frac{k}{6I(t)}. \end{aligned} \quad (12)$$

Where δt is small enough to ensure that for each m , $\langle (\Delta\hat{I}(m\delta t))^2 \rangle / I(m\delta t)^2$ can be seen as fixed in the interval $[(m-1)\delta t, m\delta t]$.

In the derivation of Eq. (12), the cross terms vanish due to the fact that $\Delta\hat{I}(m_1\delta t)$ and $\Delta\hat{I}(m_2\delta t)$ at different instants are irrelevant. Therefore, only the square terms remain. To get the final result of Eq. (12), Eq. (9) and Eq. (10) are applied, and the fact that $\sum_{m=1}^{+\infty} 1/m^2 = \pi^2/6$ and $1/I(t)$ is continuous and derivative are considered. A detailed derivation of Eq. (12) is given in the Supplement, Note 2.

Assuming the “ \parallel ” and “ \perp ” respectively represent the radical and tangential components, then $\langle (\Delta\hat{h}_\parallel)^2 \rangle$ and $\langle (\Delta\hat{h}_\perp)^2 \rangle$, which are the two orthogonal components of the radical (amplitude) and the tangential fluctuations of $h(t)$, correspondingly have the form $\Delta\hat{h}_\parallel = \Delta|\hat{h}(t)|$ and

$\Delta\hat{h}_\perp = |h(t)|\Delta\hat{\phi}(t)$ as shown in Fig. 3 (a). We thus obtain the following quantum mechanical variances for the detection of a coherent state.

$$\begin{aligned}\langle(\Delta\hat{h}_\parallel)^2\rangle &= \langle(\Delta|\hat{h}(t)|)^2\rangle = \frac{\langle[\sqrt{\hat{I}(t)} - \sqrt{I(t)}]^2\rangle}{k} \\ &\approx \frac{1}{k}\langle\left[\frac{\hat{I}(t) - I(t)}{2\sqrt{I(t)}}\right]^2\rangle = \frac{\langle(\Delta\hat{I}(t))^2\rangle}{4kI(t)} = \frac{1}{2},\end{aligned}\quad (13)$$

$$\langle(\Delta\hat{h}_\perp)^2\rangle = \frac{1}{k}\langle I(t)(\Delta\hat{\phi}(t))^2\rangle = \frac{\langle(\Delta\hat{I}(t))^2\rangle}{12kI(t)} = \frac{1}{6}. \quad (14)$$

From Eq. (8), the quantum fluctuation N of α'_s is calculated as

$$\begin{aligned}N &= \langle(\Delta\hat{\alpha}'_s)^2\rangle \\ &= \langle(\Delta\hat{h})^2\rangle |e^{j\omega_{IF}t}|^2 = \langle(\Delta\hat{h}_\parallel)^2\rangle + \langle(\Delta\hat{h}_\perp)^2\rangle = \frac{2}{3}.\end{aligned}\quad (15)$$

Considering Eq. (15), the upper limit of S/N of KK detection due to the quantum fluctuation is equal to $\frac{3}{2}\langle n_s \rangle$.

$$(S/N)_{KK} = \langle n_s \rangle / N = \frac{3}{2}\langle n_s \rangle. \quad (16)$$

In contrast, for the balanced heterodyne detection, the $(S/N)_{Bal}$ approaches $\langle n_s \rangle$ when $\langle n_L \rangle \gg \langle n_s \rangle$ as shown in Eq. (5).

From Eq. (13) and Eq. (14) we find that, with the KK relations, \hat{h}_\parallel has the radical fluctuations twice that of a coherent state, which embodies the contribution of the signal \hat{A}_s as well as the image \hat{A}_i . Meanwhile, the tangential fluctuations resulted by KK detection are only 1/3 times the radical ones. This ratio reveals the physical contribution of KK relation, which is, physically, from the Hilbert transform. The introduction of the Hilbert transform provides extra information for measuring the tangential component of the MP signal compared with direct measurement. It is the smaller tangential fluctuation that leads to a greater SNR of the KK detection than that of the balanced heterodyne detection.

The Arthurs-Kelly model [14] points out that, in order to realize the simultaneous measurement of a pair of non-reciprocal mechanical observables, two new reciprocal observables can be constructed, which have the same expected values as the former two do. Meanwhile, the total fluctuations resulted by the measurement process of the two observables constructed will be at least doubled compared with the respective measurement results of the two original observables. It can be proved that when $\langle n_L \rangle \gg \langle n_s \rangle$ holds, for the balanced heterodyne detection, as a pair of reciprocal observables constructed, the in-phase and quadrature components of $\hat{A}_s + \hat{A}_i^\dagger$ can be measured simultaneously, which contribute the same to the total fluctuations.

Different from the balanced heterodyne detection, for each signal transmitted, the KK receiver makes use of the detected intensity information of photocurrent at each time in the signal duration, to indirectly measure (calculate) the MP signal phase

$\phi(t)$. Instead of measuring the tangential component directly, KK receiver utilizes the Kramers-Kronig constraint relations between the expected value of phase at the decision time $\phi(t)$, and that of photocurrent intensity at other times $I(t')$ ($-\infty < t' < +\infty, t' \neq t$). This introduces more knowledge about phase $\phi(t)$ provided by the Hilbert transform, into the detection process, further compressing the fluctuations of measuring \hat{h}_\perp to only 1/3 times those of measuring \hat{h}_\parallel . Eq. (15) reveals that, for the KK receiver, the total quantum variance is only 2/3 compared with 1 of balanced heterodyne detection, which indicates its physical nature.

Now for the specific frequency ω , we consider the original form of KK relations depicting the correlation between transmission for the intensity $\eta(\omega)$ and phase shift $\varphi(\omega)$ (with respect to propagation in the vacuum) of light which has propagated in the medium for a limited distance [15]. Comparing Eq. (6) with Eq. (2) of [15], it is obvious that in the sense of being linked by KK relations, $\eta(\omega)$ and $\varphi(\omega)$ respectively correspond to current $I(t)$ and its phase $\phi(t)$. Through the analysis in frequency domain, the conclusion of [15] is that compared with joint phase-loss estimation such as balanced heterodyne detection, the precision of measuring the phase shift can be further improved taking into account KK relations. This is consistent with our conclusion, that is, through the KK receiver, the amplitude and phase of MP signal can be obtained at the same time, while the fluctuation of measuring phase can be compressed to 1/6, which is even less than 1/4 of directly measuring phase component of a coherent state signal. This further leads to the result that using KK relations, the SNR of the coherent state signals can achieve $\frac{3}{2}\langle n_s \rangle$, which is higher than $\langle n_s \rangle$ of balanced heterodyne detection.

As shown in Fig. 3 (b) and Fig. 3 (c), the KK receiver results in a smaller total noise energy than the conventional balanced heterodyne detection does, while the end point of the MP signal from the KK receiver has an elliptical asymmetrical distribution, indicating a specific physical essence of KK detection in quantum case.

Now we check the quantum variances of the in-phase and quadrature field operators of the signal $\langle(\Delta\hat{\alpha}'_{s1})^2\rangle$ and $\langle(\Delta\hat{\alpha}'_{s2})^2\rangle$, which represent the variances of amplitude and phase quadratures (position and momentum) of $\hat{\alpha}'_s$ respectively. From Fig. 2, by expanding $\Delta\hat{\alpha}'_s$ and $\Delta\hat{h}$, we can rewrite Eq. (8) as

$$\begin{aligned}\Delta\hat{\alpha}'_{s1} + j\Delta\hat{\alpha}'_{s2} &= (\Delta\hat{h}_\parallel \cos(\phi(t)) - \Delta\hat{h}_\perp \sin(\phi(t)))e^{j\omega_{IF}t} \\ &\quad + j(\Delta\hat{h}_\perp \sin(\phi(t)) + \Delta\hat{h}_\parallel \cos(\phi(t)))e^{j\omega_{IF}t}.\end{aligned}\quad (17)$$

Substituting the relation $e^{j\omega_{IF}t} = \cos\omega_{IF}t + j\sin\omega_{IF}t$ into Eq. (17) to extract the real and the imaginary parts respectively, we get

$$\begin{bmatrix} \Delta\hat{\alpha}'_{s1} \\ \Delta\hat{\alpha}'_{s2} \end{bmatrix} = \begin{bmatrix} \cos(\omega_{IF}t + \phi(t)) & -\sin(\omega_{IF}t + \phi(t)) \\ \sin(\omega_{IF}t + \phi(t)) & \cos(\omega_{IF}t + \phi(t)) \end{bmatrix} \begin{bmatrix} \Delta\hat{h}_\parallel \\ \Delta\hat{h}_\perp \end{bmatrix}. \quad (18)$$

Then the variances of $\langle(\Delta\hat{\alpha}'_{s1})^2\rangle$ and $\langle(\Delta\hat{\alpha}'_{s2})^2\rangle$ are calculated as

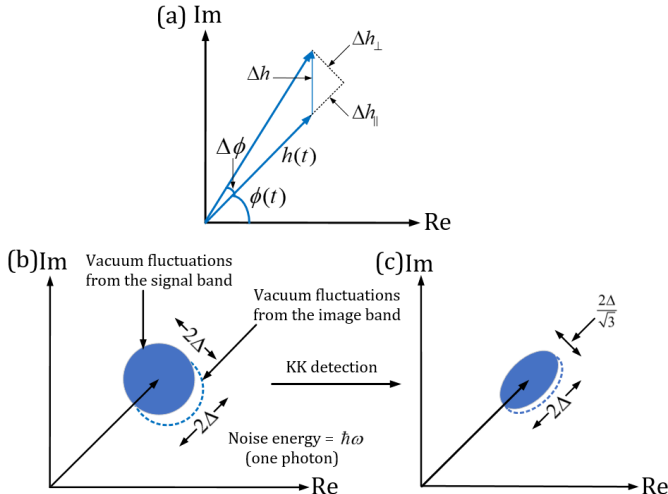


Fig. 3. Quantum noise associated with the KK receiver. (a) The radical and the tangential fluctuations; (b) Quantum noise from the signal and the image bands; (c) Phasor diagram of the light after KK detection. $\Delta=1/2$ represents the standard deviation of the quantum fluctuations of the coherent state.

$$\begin{bmatrix} \langle(\Delta\hat{\alpha}'_{s1})^2\rangle \\ \langle(\Delta\hat{\alpha}'_{s2})^2\rangle \end{bmatrix} = \begin{bmatrix} \cos^2(\omega_{IF}t + \phi(t)) & \sin^2(\omega_{IF}t + \phi(t)) \\ \sin^2(\omega_{IF}t + \phi(t)) & \cos^2(\omega_{IF}t + \phi(t)) \end{bmatrix} \begin{bmatrix} \langle(\Delta\hat{h}_{\parallel})^2\rangle \\ \langle(\Delta\hat{h}_{\perp})^2\rangle \end{bmatrix}. \quad (19)$$

Eq. (19) is obtained using the relation $\langle\Delta\hat{h}_{\parallel}\Delta\hat{h}_{\perp}\rangle = 0$.

Note that 'T' stands for matrix transposition. Eq. (19) shows that $\langle(\Delta\hat{\alpha}'_{s1})^2\rangle, \langle(\Delta\hat{\alpha}'_{s2})^2\rangle$ are related to $\langle(\Delta\hat{h}_{\parallel})^2\rangle, \langle(\Delta\hat{h}_{\perp})^2\rangle$ through a transformation matrix determined by $\omega_{IF}t + \phi(t)$, which brings no physical discrepancy between the fluctuation distributions of $\hat{\alpha}'_s$ and \hat{h} . As shown in Eq. (13) and Eq. (14), three times difference between $\langle(\Delta\hat{h}_{\parallel})^2\rangle$ and $\langle(\Delta\hat{h}_{\perp})^2\rangle$ results in the asymmetric distribution of $\langle(\Delta\hat{\alpha}'_s)^2\rangle$. For the retrieved $\hat{\alpha}'_s$, with the total fluctuations kept the same as those of \hat{h} , the in-phase and quadrature fluctuations both have a time dependent evolution as a function of $\omega_{IF}t + \phi(t)$. In other words, there exists a time varying accuracy for the measured position and momentum components of a coherent signal using the KK receiver. From Fig. 2, we can see that for a given α_s , the time varying of the projected in-phase and quadrature field fluctuation is related to the phase evolution of $\omega_{IF}t$. The time-varying property of $\langle(\Delta\hat{\alpha}'_{s1})^2\rangle, \langle(\Delta\hat{\alpha}'_{s2})^2\rangle$ essentially results from the factor $e^{i\omega_{IF}t}$ in Eq. (7), in which t as the decision time is selected artificially. This means that based on measuring \hat{h} through the KK receiver, additional mathematical constraints are added to further recover α'_s .

For instance, Fig. 4 shows the phasor diagram of the retrieved signal α'_s at four specific orientations for a coherent state. In contrast to the conventional balanced heterodyne or homodyne detection, the KK receiver exhibits asymmetric quantum noise in both in-phase and quadrature operators that depends on the time varying phase of $\omega_{IF}t + \phi(t)$ when it is applied to measure a coherent state.

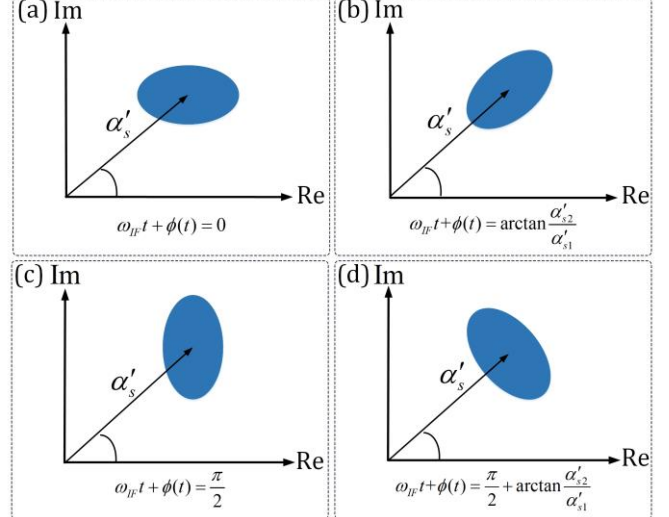


Fig. 4. Phasor diagram of the retrieved signal α'_s at four specific orientations for a coherent state.

Combing Fig. 2 and Fig. 4, it can be seen that when $\sqrt{1-\varepsilon}\alpha_L \gg \alpha_s$ holds, there will hold $\phi(t) \approx 0$ no matter how t varies. Consequently, the phase term $\omega_{IF}t + \phi(t)$ will be approximately equal to $\omega_{IF}t$. Since t is defined as the decision time while ω_{IF} represents the intermediate frequency, both of which are known varieties. In principle, we can control the fluctuation distribution by reasonably selecting these two variables. Therefore, the quantum fluctuation of the electromagnetic field can be compressed to 1/6 in the specific direction selected to be measured more accurately.

5. SIMULATION RESULTS

To validate our analytical derivation and illustrate the statistical nature of quantum fluctuations of KK detection, we perform numerical simulation with up to 40000 signals which are detected with the KK receiver. Without losing generality, the Quadrature Phase Shift Keying (QPSK) modulation format is selected in the simulation for simplicity.

To approximate the KK relations, Eq. (6) is discretized into the form of Riemann sum. With the signal duration T selected as the integral interval, to approach the condition $\delta t \rightarrow 0$ (relative to T) in Eq. (12), up to 2×10^5 sampling points are selected to realize $\delta t = T/(2 \times 10^5)$. While the decision time t is set as $t = T/2$ to keep the integral intervals on both sides of t symmetrical.

Since the Poisson distribution can be approximated by

Gaussian distribution as its mean becomes large [16], Gaussian random number is used to simulate the measured noise. At the same time, by adding the current noise at each time point independently, the Gaussian white noise property is satisfied.

Thus to model the fluctuations of current $\langle(\Delta\hat{I}(t))^2\rangle_{KK}$, as has been proved in the Supplement, Eq. (S5), we may as well assume that the current deviation $\Delta I(t)_{KK}$ has the following form for carrying out the simulation using MATLAB.

$$\Delta I(t)_{KK} = \sqrt{2k\langle\hat{I}(t)\rangle_{KK}} \times \text{randn} . \quad (20)$$

Where ‘randn’ represents the Gaussian random number with the mean value as 0 and the standard deviation as 1, thus the quantum noise of $I(t)_{KK}$ at time point t is modeled as the independent Gaussian noise with 0 mean and variance equaling to $2k\langle\hat{I}(t)\rangle_{KK}$.

The carrier to signal power ratio (CSPR) of the MP signal can be defined as

$$\text{CSPR} \triangleq \frac{|\sqrt{1-\varepsilon}\alpha_L|^2}{|\sqrt{\varepsilon}\alpha_s|^2} = \frac{(1-\varepsilon)\langle n_L \rangle}{\varepsilon\langle n_s \rangle} > 1 . \quad (21)$$

First, we set CSPR to 10 dB and let $\langle n_s \rangle$ start from 20 and increase in a step of 20. For QPSK signals, it can be seen that the fluctuations surrounding each constellation point showed an asymmetric elliptical distribution on the constellation plane as we have predicted in our derivations (Supplement, Note 3).

Each received constellation point represents the recovered α'_s in Eq. (7) normalized by $\sqrt{\langle n_s \rangle/2}$. With $\langle n_s \rangle$ increasing, the fluctuations surrounding each constellation point decreases. Moreover, the simulation results (Supplement, Note 4) for the constellations with $\text{CSPR} = 10 \text{ dB}$ & $\langle n_s \rangle$ varying from 20 to 200 are concluded in Fig. 5 (a) & Fig. 5 (b), in which the square of the ratio of the major axis to the minor one of fluctuation ellipse is defined as ρ_{KK} .

Fig. 5 (a) shows ρ_{KK} in four quadrants calculated by principal component analysis method provided by MATLAB. Fig. 5 (b) shows the calculated SNR of the received QPSK signals based on KK receiver for different $\langle n_s \rangle$. As shown in Fig. 5 (a), the ρ_{KK} of the simulation results is almost consistent with the predicted value 3/1. While Fig. 5 (b) indicates that for KK receiver, the SNR of the signal is proportional to its photon number $\langle n_s \rangle$, which shows approximately a linear correlation of $\text{SNR} = \frac{3}{2}\langle n_s \rangle$. The simulative results of Fig. 5 (a) and Fig. 5 (b) are consistent with our analytic conclusions Eq. (13), Eq. (14) & Eq. (16).

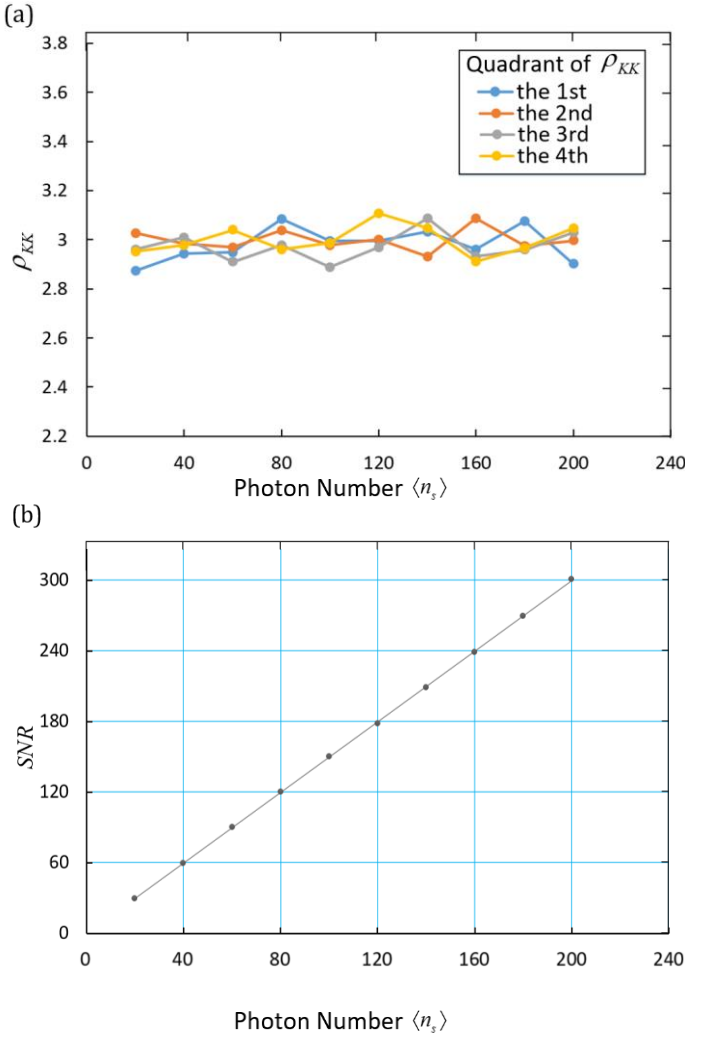


Fig. 5. The analysis results for the constellations with $\text{CSPR} = 10 \text{ dB}$ & $\langle n_s \rangle$ varying from 20 to 200.

(a) ρ_{KK} of each quadrant;(b)The Relation Between SNR and $\langle n_s \rangle$.

Fixing $\langle n_s \rangle$ as 100 and $\omega_{IF}t \bmod T_{IF} = 0$, Fig. 6 illustrates the constellation diagram of the retrieved signal α'_s with the CSPR set as 5 dB, 10 dB, 15 dB and 20 dB, respectively. The horizontal and vertical coordinates of the constellations respectively represent the in-phase and quadrature components of α'_s recovered through Eq.(7). As shown in Fig. 6, with the CSPR increasing, the direction of the major axis of the fluctuation ellipse in each quadrant, tends to be consistent with the direction of the carrier as predicted at the end of Section IV. This implies that when the CSPR is large enough ($(1-\varepsilon)\langle n_L \rangle \gg \varepsilon\langle n_s \rangle$ holds), the distribution of the fluctuations will be determined by $\omega_{IF}t$ almost completely.

For the simulation of the four cases predicted in Fig. 4, the CSPR is set as 30 dB to meet the condition $(1-\varepsilon)\langle n_L \rangle \gg \varepsilon\langle n_s \rangle$. Fig. 7 (a)-(d) show the constellations of α'_s when the decision time t is selected to meet the conditions

$$\omega_{IF}t \bmod T_{IF} = 0, \frac{\pi}{4}, \frac{\pi}{2} \text{ & } \frac{3\pi}{4}, \text{ respectively.}$$

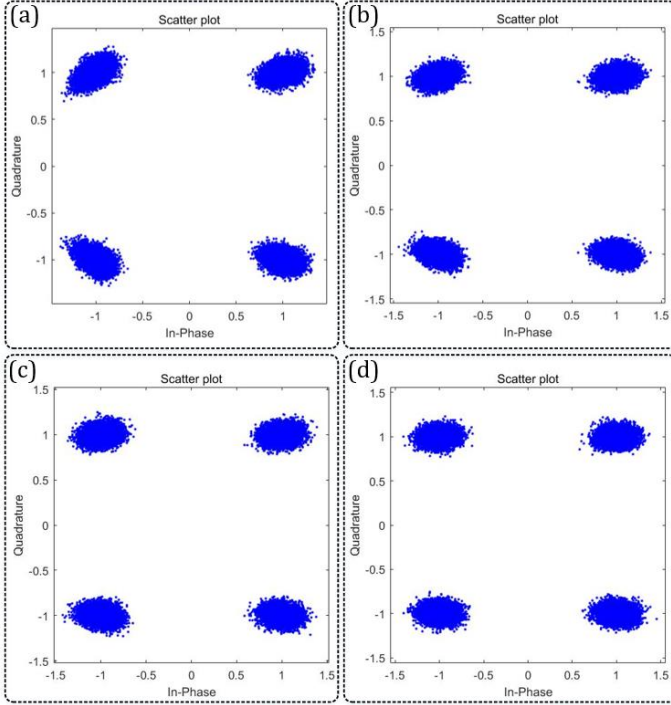


Fig. 6. The constellations of α'_s for different *CSPR* values with $\langle n_s \rangle = 100$ and $\omega_{IF}t \bmod T_{IF} = 0$

(a) *CSPR* = 5 dB ;(b) *CSPR* = 10 dB ;(c) *CSPR* = 15 dB ;(d) *CSPR* = 20 dB

As shown in Fig. 7 (a) and Fig. 7 (c), we can either compress the in-phase or quadratic fluctuation to only 1/6, while keeping that of the other orthogonal direction at 1/2. In Fig. 7 (b) and Fig. 7 (d), the fluctuation of both in-phase and quadratic components can be compressed to 1/3 at the same time. The results indicate that for high *CSPR* such as $CSPR \geq 30$ dB, the KK receiver can achieve a high controllability of the fluctuation distribution on the constellation plane. This is implemented by selecting the phase term $\omega_{IF}t$ according to the accuracy requirements for the specific direction to be measured.

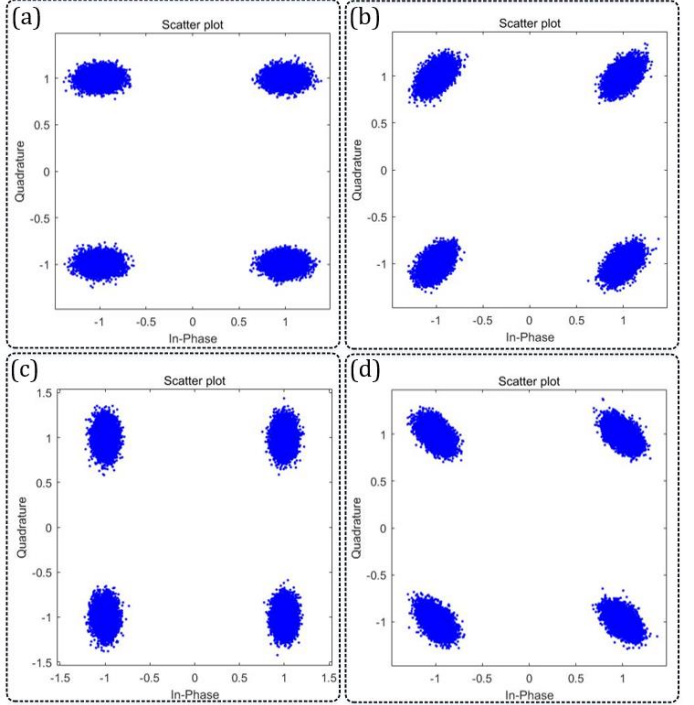


Fig. 7. The received constellations of different decision time *t* with $\langle n_s \rangle = 100$ and *CSPR* = 30dB

(a) $\omega_{IF}t \bmod T_{IF} = 0$;(b) $\omega_{IF}t \bmod T_{IF} = \frac{\pi}{4}$;

(c) $\omega_{IF}t \bmod T_{IF} = \frac{\pi}{2}$;(d) $\omega_{IF}t \bmod T_{IF} = \frac{3\pi}{4}$

6. CONCLUSION

In summary, we analytically derive the quantum noise of the in-phase and quadrature operators of the retrieved coherent-state signal with the KK receiver. The quantum limit of the *SNR* of the KK receiver is 3/2 times the expectation value of the signal photon number. Therefore, the KK receiver has a larger *S/N* limit than that of balanced heterodyne detection. This is consistent with the conclusion of [15]. Since the intensity of the MP signal is physically measured, while its phase is calculated from the intensity using Kramers-Kronig relations, KK receiver keeps the tangential noise to 1/3 times that of the amplitude, further leading to an asymmetric distribution of the quantum fluctuation of the retrieved signal. The projected variances of the in-phase and quadrature operators are time-varying due to the phase evolution of the intermediate frequency, which provides us a scheme using a high *CSPR* to measure the component of a specific direction with fluctuations compressed to 1/6. The analytical conclusions is validated by numerical simulation. Our work provides a physical insight of the KK receiver and should enrich the knowledge of electromagnetic noise in quantum optical measurement.

Funding.

National Natural Science Foundation of China (62271010, U21A20454 and 11834010); National Key Research and Development Program of China (2018YFB1801204 and 2016YFA0301402).

Acknowledgment.

Disclosures.

The authors declare no competing interests.

Data availability.

Data underlying the results presented in this paper are not publicly available at this time but may be obtained from the authors upon reasonable request.

Supplemental document.

See Supplement for supporting content.

REFERENCES

1. K. Kikuchi, "Fundamentals of coherent optical fiber communications," *J. Lightwave Technol.* **34**, 157-179 (2016).
2. A. Mecozzi, C. Antonelli, and M. Shtaif, "Kramers-Kronig coherent receiver," *Optica* **3**, 1220-1227 (2016).
3. A. Mecozzi, C. Antonelli, and M. Shtaif, "Kramers-Kronig receivers," *Adv. Opt. Photon.* **11**, 480-517 (2019).
4. X. Chen, C. Antonelli, S. Chandrasekhar, G. Raybon, A. Mecozzi, M. Shtaif, and P. Winzer, "Kramers-Kronig receivers for 100-km datacenter interconnects," *J. Lightwave Technol.* **36**, 79 – 89 (2018).
5. S. T. Le, K. Schuh, R. Dischler, F. Buchali, L. Schmalen, and H. Buelow, "Beyond 400 Gb/s direct detection over 80 km for data center Zinterconnect applications," *J. Lightwave Technol.* **38**, 538-545 (2020).
6. S. L. Braunstein, and P. van Loock, "Quantum information with continuous variables," *Rev. Mod. Phys.* **77**, 513-577 (2005).
7. G. Adesso and F. Illuminati, "Entanglement in continuous-variable systems: recent advances and current perspectives," *J. Phys. A: Math. Theor.* **40**, 7821-7880 (2007).
8. X. -B. Wang, T. Hirishima, A. Tomita, and M. Hayashi, "Quantum information with Gaussian states," *Phys. Rep.* **448**, 1-111 (2007).
9. C. Weedbrook, S. Pirandola, R. García-Patrón, N. J. Cerf, T. C. Ralph, J. H. Shapiro, and S. Lloyd, "Gaussian quantum information," *Rev. Mod. Phys.* **84**, 621-669 (2012).
10. X. Su, M. Wang, Z. Yan, X. Jia, C. Xie, and K. Peng, "Quantum network based on non-classical light," *Sci. China Inf. Sci.* **63**, 180503 (2020).
11. Y. Yamamoto and H. A. Haus, "Preparation, measurement and information capacity of optical quantum states," *Rev. Mod. Phys.* **58**, 1001-1020 (1986).
12. M. O. Scully and M. S. Zubairy, "quantum phase and amplitude fluctuations," in *Quantum Optics* (Cambridge University Press, 1997), Ch. XIV, pp. 423-426.
13. H. A. Haus, *Electromagnetic Noise and Quantum Optical Measurements* (Berlin Heidelberg, Springer-Verlag, 2000), Ch. VIII, pp. 281-304.
14. E. Arthurs and J. L. Kelly, "B.S.T.J. briefs: on the simultaneous measurement of a pair of conjugate observables," *The Bell System Technical Journal* **44**, 725-729 (1965).
15. I. Gianani, F. Albarelli, A. Verna, V. Cimini, R. Demkowicz-Dobrzanski, and M. Barbieri, "Kramers-Kronig relations and precision limits in quantum phase estimation," *Optica* **8**, 1642-1645 (2021).
16. W. Feller, "laws of large numbers," in *An Introduction to Probability Theory and its Applications*, 3rd ed. (John Wiley & Sons, Inc, 1968), Vol. I, Ch. X, pp. 245-246.

Quantum Noise of Kramers-Kronig Receiver

FAN ZHANG,¹ JIAYU ZHENG,¹ HAIJUN KANG,² XIAOLONG SU,² AND QIONGYI HE³

¹ State Key Laboratory of Advanced Optical Communication System and Networks, Frontiers Science Center for Nano-optoelectronics, Department of Electronics, Peking University, Beijing 100871, China

² State Key Laboratory of Quantum Optics and Quantum Optics Devices, Institute of Opto-Electronics, Collaborative Innovation Center of Extreme Optics, Shanxi University, Taiyuan 030006, China

³ State Key Laboratory for Mesoscopic Physics, School of Physics, Frontiers Science Center for Nano-optoelectronics & Collaborative Innovation Center of Quantum Matter, Peking University, Beijing 100871, China

*xyz@optica.org

Supplementary Note 1: The general proof of the relation of Eq. (9) and Eq. (10)

Here we give a general proof of the relation of Eq. (9) and Eq. (10) in the main text. Considering an operator \hat{I} that measures the intensity of the electrical field consisting of N different frequency modes \hat{A}_u ($u=1, \dots, N$), we have

$$\hat{I} = \left(\sum_{u=1}^N \lambda_u \hat{A}_u \right)^\dagger \left(\sum_{u=1}^N \lambda_u \hat{A}_u \right). \quad (\text{S1})$$

λ_u is the strength of \hat{A}_u . We have the following commutation relation as

$$\sum_{u=1}^N \lambda_u^2 = \left[\left(\sum_{u=1}^N \lambda_u \hat{A}_u \right), \left(\sum_{u=1}^N \lambda_u \hat{A}_u \right)^\dagger \right] = r. \quad (\text{S2})$$

Considering the expression that the operator \hat{I}^2 minus the normally ordered operator of \hat{I}^2 , we have

$$\begin{aligned} \hat{I}^2 - :\hat{I}^2: &= \left[\left(\sum_{u=1}^N \lambda_u \hat{A}_u \right)^\dagger \left(\sum_{u=1}^N \lambda_u \hat{A}_u \right) \right]^2 \\ &\quad - \left[\left(\sum_{u=1}^N \lambda_u \hat{A}_u \right)^\dagger \right]^2 \left[\left(\sum_{u=1}^N \lambda_u \hat{A}_u \right) \right]^2 \\ &= \left(\sum_{u=1}^N \lambda_u \hat{A}_u \right)^\dagger \left[\left(\sum_{u=1}^N \lambda_u \hat{A}_u \right), \left(\sum_{u=1}^N \lambda_u \hat{A}_u \right)^\dagger \right] \left(\sum_{u=1}^N \lambda_u \hat{A}_u \right) \\ &= \left(\sum_{u=1}^N \lambda_u \hat{A}_u \right)^\dagger \left(\sum_{u=1}^N [\hat{A}_u, \hat{A}_u^\dagger] \lambda_u^2 \right) \left(\sum_{u=1}^N \lambda_u \hat{A}_u \right) \\ &= r \left(\sum_{u=1}^N \lambda_u \hat{A}_u \right)^\dagger \left(\sum_{u=1}^N \lambda_u \hat{A}_u \right) \end{aligned} \quad (\text{S3})$$

Here $:\hat{I}^2:$ represents the normally ordered \hat{I}^2 only including the terms with the creation operators preceding the annihilation operators.

The expectation of $\hat{I}^2 - :\hat{I}^2:$ equals to the fluctuations $\langle (\Delta \hat{I})^2 \rangle$ in the measurement of \hat{I} . We have

$$\begin{aligned} \langle (\Delta \hat{I})^2 \rangle &= \langle \hat{I}^2 - :\hat{I}^2: \rangle \\ &= r \langle \left(\sum_{u=1}^N \lambda_u \hat{A}_u \right)^\dagger \left(\sum_{u=1}^N \lambda_u \hat{A}_u \right) \rangle. \\ &= r \langle \hat{I} \rangle \end{aligned} \quad (\text{S4})$$

As for $\hat{h} = \sqrt{1-\varepsilon}(\hat{A}_L + \hat{A}_s' + \hat{A}_i') + \sqrt{\varepsilon}(\hat{A}_s + \hat{A}_i)$ ($\varepsilon \rightarrow 1$) in our paper, we have $N = 5$ and $r = \sum_{u=1}^N \lambda_u^2 = 3(1-\varepsilon) + 2\varepsilon = 3 - \varepsilon \rightarrow 2$.

Therefore, for $\hat{I}(t)_{KK} = k\hat{h}^\dagger \hat{h}$, we obtain

$$\langle (\Delta \hat{I}(t))^2 \rangle_{KK} = 2k \langle \hat{I}(t) \rangle_{KK}. \quad (\text{S5})$$

Eq. (10) in the main text can thus be readily obtained from Eq. (9) through the relation that is revealed in Eq. (S5).

Supplementary Note 2: The derivation of Eq. (12)

Here we give the derivation of Eq. (12) in the main text. Note that Eq. (11) can be used to calculate the phase fluctuations.

$$\langle(\Delta\hat{\phi}(t))^2\rangle = \frac{1}{4\pi^2} \left\langle \left\{ \mathcal{P} \int_{-\infty}^{+\infty} \frac{1}{t-t'} \left[\frac{\hat{I}(t') - I(t')}{I(t')} \right] dt' \right\}^2 \right\rangle \quad (S6)$$

Let $t = l\delta t$, $t' = m\delta t$ and $dt' \rightarrow \delta t$, then Eq. (S6) can be rewritten as the following discrete form. To bypass the singularity of the integrand, $m \neq l$.

$$\langle(\Delta\hat{\phi}(t))^2\rangle = \lim_{\delta t \rightarrow 0} \frac{1}{4\pi^2} \left\langle \left\{ \sum_{m=-\infty, m \neq l}^{m=+\infty} \frac{1}{l\delta t - m\delta t} \left[\frac{\Delta\hat{I}(m\delta t)}{I(m\delta t)} \right] \right\}^2 (\delta t)^2 \right\rangle \quad (S7)$$

Due to the white noise property, the measurement of $\Delta\hat{I}$ at different instants $m_1\delta t$ and $m_2\delta t$ are irrelevant. Considering the cross terms in the summation in Eq. (S7), we have

$$\begin{aligned} & \lim_{\delta t \rightarrow 0} \frac{1}{4\pi^2} \left\langle \sum_{m_1, m_2} \frac{1}{(l-m_1)(l-m_2)} \frac{\Delta\hat{I}(m_1\delta t)\Delta\hat{I}(m_2\delta t)}{I(m_1\delta t)I(m_2\delta t)} \right\rangle \\ &= \lim_{\delta t \rightarrow 0} \frac{1}{4\pi^2} \sum_{m_1, m_2} \frac{1}{(l-m_1)(l-m_2)} \frac{\langle\Delta\hat{I}(m_1\delta t)\rangle\langle\Delta\hat{I}(m_2\delta t)\rangle}{I(m_1\delta t)I(m_2\delta t)} \\ &= 0 \end{aligned} \quad (S8)$$

Therefore, the cross terms vanish and only the square terms remain. We can thus rewrite $\langle(\Delta\hat{\phi}(t))^2\rangle$ as

$$\begin{aligned} \langle(\Delta\hat{\phi}(t))^2\rangle &= \lim_{\delta t \rightarrow 0} \frac{1}{4\pi^2} \left[\sum_{m=-\infty}^{m=l-1} \frac{1}{(l-m)^2} \frac{\langle(\Delta\hat{I}(m\delta t))^2\rangle}{I(m\delta t)^2} \right. \\ &\quad \left. + \sum_{m=l+1}^{+\infty} \frac{1}{(l-m)^2} \frac{\langle(\Delta\hat{I}(m\delta t))^2\rangle}{I(m\delta t)^2} \right]. \end{aligned} \quad (S9)$$

We introduce Eq. (9) and Eq. (10) in the main text into Eq. (S9) and consider Eq. (S5) in the derivation of Eq. (12) in the main text. Note that $\sum_{m=1}^{+\infty} 1/m^2 = \pi^2/6$, the final result of Eq. (12) in the main text is thus obtained.

Supplementary Note 3: The received constellations with $\langle n_s \rangle = 60, 100, 160, 200$ corresponding to Fig. 5 (b)

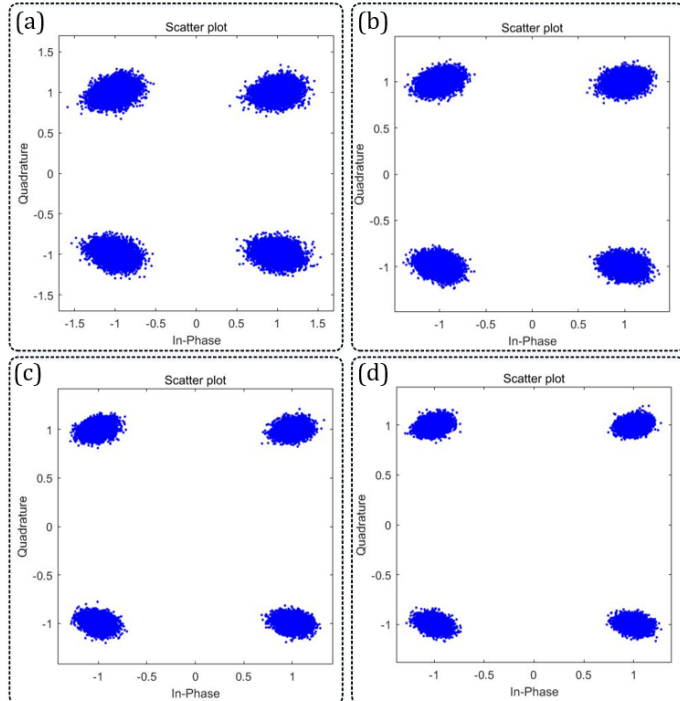


Fig. S1. The received constellations of different $\langle n_s \rangle$ with $CSPR = 10\text{dB}$.

(a) $\langle n_s \rangle = 60$; (b) $\langle n_s \rangle = 100$; (c) $\langle n_s \rangle = 160$; (d) $\langle n_s \rangle = 200$.

Supplementary Note 4: ρ_{KK} & SNR varying with $\langle n_s \rangle$ corresponding to Fig. 5 (a) & (b)

Table. S1. The ρ_{KK} result of each quadrant from 1 to 4 for different $\langle n_s \rangle$

$\langle n_s \rangle$	ρ_{KK} of 1-4 quadrant			
	1	2	3	4
20	2.874706	3.027615	2.961494	2.951422
40	2.94412	2.982373	3.008735	2.977746
60	2.949367	2.969697	2.909735	3.039497
80	3.083189	3.037461	2.978155	2.960401
100	2.996097	2.978788	2.888889	2.985119
120	2.99639	3	2.967857	3.107914
140	3.032097	2.93051	3.086325	3.045746
160	2.959388	3.086683	2.931786	2.910781
180	3.074675	2.973712	2.95883	2.965812
200	2.901145	2.996441	3.028863	3.046667

Table. S2. The SNR result for different $\langle n_s \rangle$

$\langle n_s \rangle$	20	40	60	80	100	120	140	160	180	200
SNR	29.72	59.46	90.17 5	120.3 47	150.4 41	178.5 06	208.9 83	238.9 55	269.3 58	300.6 92

Table. S1, S2.